Cytoplasmic streaming in *C. elegans* : forces that drive oogenesis

Vidya V. Menon[1], Mandar M. Inamdar[*2], and Anirban Sain[**3]

[1]Center for Research in Nano Technology and Science,
[2] Department of Civil Engineering and [3]Physics Department,
Indian Institute of Technology-Bombay, Powai, Mumbai, 400076, India.

[**]asain@phy.iitb.ac.in, [*]minamdar@iitb.ac.in

Abstract

In the gonad of *C. elegans* worms, germ cells form the outer lining of the central tube, the rachis, which carries a cytoplasmic flow. The porous interface between the germ cells and rachis allows a radial flow of cytoplasm across the interface. In the upstream, the flow at the interface is radially inwards boosting the main cytoplasmic flow in the rachis, while in the downstream the flow is radially outward feeding the germ cells to become oocytes. We analyze the cytoplasmic flow in rachis as a flow in a porous tube of varying width, with spatially heterogeneous flow injection or leakage rates. Taking the geometry of the rachis into account, we predict properties of the rachis flow, such as pressure gradients and spatially heterogeneous flow speeds. Based on these, we speculate how directions of sub-flows between germ cells and rachis could be regulated for the development of healthy oocytes. Knowledge of this connection between micro-scale flow mechanics and physiological parameters may then also help us understand the abnormalities of reproduction in *C. elegans* worms with mutations or pathologies.

1 Introduction

Cytoplasmic streaming is responsibe for fast transport of nutrients, filaments, mRNA and other material from one part of the cell or organ to the other [8]. Some examples are, movements of chloroplasts and growth of pollen tubes in plants, and intra-cellular transport of actin monomers in the direction of cell movement [10]. Oogenesis, the mechanism for production of egg cells or oocytes in *C. elegans* worms offers a model system to understand how cytoplasmic streaming nourish potential oocytes, required for reproduction. While this model system has been important to developmental biologists for studying stem cell differentiation, programmed cell death (apoptosis) and embryo development [11, 20, 7], we are interested in the mechanical aspects of cytoplasmic streaming. Specifically, we seek to estimate the magnitude and direction of pressure gradients within the *C. elegans* gonad that are needed to sustain cytoplasmic streaming and the closely associated oocyte production, at experimentally observed rates.

The reproductive system of *C. elegans* has two identical U-shaped gonad tubes extending from a single vulva (see fig. 1a)) [13, 5]. One of the U shaped arms, with the proximal and distal ends marked, is schematically shown in fig. 1b) in greater details [14]. The arm consists of an inner central tube called rachis [13, 1], which has a corset-like structure with a regular array of holes called rachis bridges [24]. These bridges connect the rachis with the germ cells that form the outer lining of the tube (see fig. 1a)). Mitotic cell divisions occur at the distal end of rachis and create a proliferation pressure gradient that drives the slow movement of the germline cells away from the distal end [5]. The main flow in the rachis, on its way to the proximal end, receives cytoplasm from the germ cells through the rachis bridges [1]. Furthermore, a significant fraction of germ cells undergo apoptosis in the late pachytene region (see fig. 1a)) and add their cytoplasm to the rachis, thereby boosting the flow [11, 26]. A somewhat similar mechanism, in which dying germ cells act as nurse cells to feed growing oocytes, has been well studied in *Drosophila* [27, 25].

A role reversal occurs towards the proximal end in that the surviving germ cells, instead of boosting the rachis flow, start to grow themselves from the cytoplasmic influx into them from the rachis, (see fig. 1). Based on this observation, Wolke *et al.* [31] proposed a few qualitative scenarios on how actomyosin contractility of the growing oocytes may assist them in pulling in cytoplasm from the rachis to grow in size. These specific flow directions require that the

pressure in the rachis must be lower than that in the nursing germline cells whereas the pressure in the growing oocytes must be lower than that in the rachis. Unidirectional flow in the rachis, on the other hand, requires a monotonically decreasing pressure in the flow direction.

There are very few instances of quantitative modeling [5, 17, 2] in this context. All the models so far focused on computation of cellular fluxes in the germline layer, lining the rachis. They used various experimentally known rates of fertilization, death, and division as inputs. Attempts have been made to connect cell speeds in the germline to protein signalling, gonad growth and ovulation cycles. However in all these the cytoplasmic streaming in the rachis has been completely ignored. In this paper, we develop a quantitative model that connects the oogenesis rate to the cytoplasmic streaming speed in the gonad and obtain the pressure gradient across the rachis required to maintain it. The model also incorporates experimentally observed spatial variations in the cytoplasmic exchange between the germline cells and rachis (see fig. 1).

We use the experimentally known parameters for the cytoplasmic flow, approximate geometry of the rachis, size of oocytes, and time-scales of ovulation to set up a quantitative model which allows us to estimate the fluid pressure profile in the streaming cytoplasm. We first model the cytoplasmic streaming through the rachis as fluid flow in a tube with porous walls [32]. The porous wall admits influx of fluid through the first part of the tube and allows outflux in its later part (fig. 1b)) thereby mimicking the influx of cytoplasm into the rachis from the germline cells and the outflux of cytoplasm into the oocytes. We do not explicitly consider the movement of germline cells and the oocytes but account for their effects on the rachis streaming only through the boundary conditions. With these assumptions, we then solve the resulting partial differential equations (PDE) for the stokes flow, using finite element analysis. We aim to obtain the pressure gradients in the rachis that can sustain these cytoplasmic exchanges and flows. We then connect proximal cytoplasmic streaming with both the size and growth rate of oocytes, as well as rachis geometry and also obtain a relation between the oocyte wall curvature and internal pressure using Young-Laplace equation. We estimate that the overall pressure drop within the rachis is relatively small when compared to the pressure difference across the cells in the germline layer. We hence propose that the pressure difference between the rachis and the surrounding cells is the primary driver of cytoplasmic streaming and thus of central importance for oogenesis in *C. elegans*.

2 Model for cytoplasmic streaming in the rachis

The influx of cytoplasm into the rachis occurs from the surrounding germline cells through the rachis bridges. Large contributions also come from apoptosis of many germline cells that are located around the turn region of the gonad [11, 26]. Germline cells that escape apoptosis are typically designated to become oocytes, and they grow rapidly by absorbing a part of the cytoplasm from the rachis flow, while slowly moving towards the proximal end of the gonad (see fig. 1a))

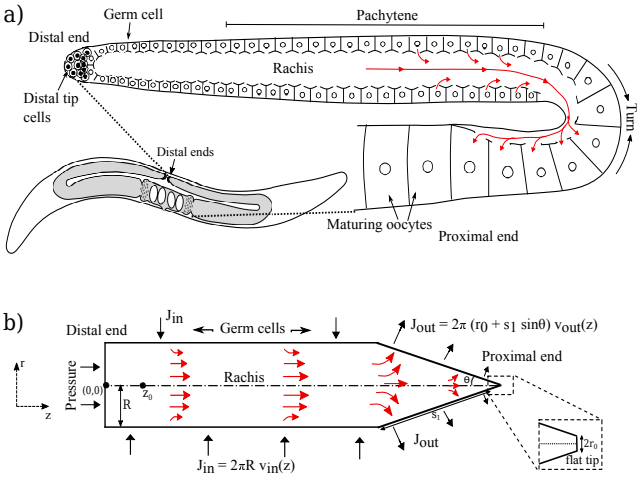

Figure 1. **Schematic diagram of the model.** a) This figure represents in detail the organisation of one of the two arms of the *C. elegans* adult hermaphrodite gonad. The shared cytoplasm called rachis is sorrounded by germ cells, some of which mature from the late pachytene region and become oocytes. The distal end of the tube where distal tip cells (DTC) are present is the end from where the flow begins and that continues till the proximal end where oocytes mature by feeding the germ cells. b) Our model to study the cytoplasmic flow inside the rachis. Model is 2D axisymmetric along the z axis and the total velocity flux is conserved in the system. The inset shows that we considered a tiny flat tip of the cone to avoid the singularity arising in the simulation due to sharp tip.

We model the cytoplasm to be incompressible as a consequence of which $\nabla \cdot \mathbf{v} = 0$, where $\mathbf{v}(\mathbf{r})$ is the velocity field for the rachis flow. The Reynolds number for the flow is $\mathrm{Re} = \frac{vR\rho}{\mu}$, where v, R, ρ, and μ are, respectively, flow speed, rachis radius, cytoplasm density, and fluid viscosity. Upon substituing the typical values for these quanti-

ties $v \approx 7\,\mu\mathrm{m/min}$, $R \approx 7\,\mu\mathrm{m}$, $\mu \approx 1\,\mathrm{Pa.s}$, and $\rho \approx 1000\,\mathrm{kg/m^3}$ [7, 16, 21, 28], we obtain $\mathrm{Re} \approx 10^{-10} \ll 1$. With these considerations, we can now describe the cytoplasmic streaming in the rachis as an axisymmetric viscous Stokes flow in a porous tube with influx/outflux boundary conditions at the walls mimicking the fluid exchange at the rachis bridges. To mimic the tapering of rachis tube towards the proximal end, we consider a composite geometry of a cylinder joined with a cone. The cylinder represents the distal arm and has length $L_{\mathrm{cyl}} = 270\,\mu\mathrm{m}$ and radius $R = 7\,\mu\mathrm{m}$. The cone represents the post-pachytene region of the rachis which gradually narrows down and ends at a maturing oocyte, see fig. 1b). We take a length $L_{\mathrm{cone}} = 90\,\mu\mathrm{m}$ for this portion. These numbers are typical of a normal, adult hermaphrodite as measured in refs. [1, 2, 31]. Also, for simplicity, we considered a straight rachis tube ignoring the post pachytene turn, (see fig. 1a)). We also assume the system to be in a steady-state in a mean sense over one oogenesis cycle, thus neglecting any finer temporal variations. The resulting equations to be solved are,

$$\nabla \cdot [-p\mathbf{I} + \mu(\nabla \mathbf{v} + (\nabla \mathbf{v})^{\mathbf{T}})] = 0, \quad \text{and} \qquad (1)$$

$$\nabla \cdot \mathbf{v} = 0, \qquad (2)$$

where, μ is the dynamic viscosity, $p(\mathbf{r})$ the pressure and $\mathbf{v}(\mathbf{r}) = (v_r, v_\theta = 0, v_z)$ is the axisymmetric velocity field for the streaming cytoplasm in cylindrical coordinates. We set flow influx boundary condition (BC) at the cylindrical portion of the wall and outflux condition at the conical region of the wall by providing normal velocity $v_n = \mathbf{v} \cdot \hat{\mathbf{n}} - v_n$ is termed v_{in} and v_{out}, respectively, for influx and outflux. The conical region in the model is terminated with a short vertical tip, and provided with zero velocity BC, to avoid convergence issues at a strictly sharp tip (see fig. 1b)). We explore various spatial distribution of $v_n(z)$ such that the total influx and outflux balance each other in this self-sustained system. In fact by simple mass conservation, the total influx of cytoplasm into the rachis should equal the volume rate at which the oocytes detach off at the end of the rachis. To prevent convergence issues that can arise from implementing this overall zero flux condition in an incompressible fluid, pressure BC $p(z = 0) = P_0$ is applied at the left extreme – the exact value of P_0 is immaterial as far as the rachis flows are concerned. The tangential velocity of the cytoplasm at the boundary is kept as zero, though strictly speaking its value should be equal to the speed of the slowly moving germline cells around the rachis. The numerical solution is obtained using the finite element analysis (FEA) software COMSOL (https://www.comsol.com).

3 Results

In the light of known experimental findings [31, 24], we now analyze our model for different combinations of influx and outflux conditions at the walls and obtain the resulting flows and pressure drops in key regions of the gonad.

3.1 Fluid pressure and flow in the cylinder for uniform boundary influx

First, we focus on spatially uniform influx because significant insight on pressure gradients can be obtained from an analytical solution known for steady laminar flows in porous cylindrical tubes [32]. This problem was originally solved for rectangular geometry by Berman [4] and was subsequently extended to cylindrical geometry by Yuan *et al.* [32]. This analytical solution also offered us a limiting case for validating our COMSOL code which can take into account more general in-/out- flux conditions and geometries, and are discussed in the results section. Yuan's expressions for pressure drop along the flow direction and the corresponding velocity profile, respectively, at low Reynolds number are

$$\Delta p(z) = \frac{4\mu v_0}{R}\left(\frac{\Delta z}{R}\right)\left[1 + \frac{2v_{\mathrm{in}}}{v_0}\frac{\Delta z}{R}\right] \text{ and } \qquad (3)$$

$$v_z(r,z) = v_0\left[1 + \frac{4v_{\mathrm{in}}}{v_0}\frac{\Delta z}{R}\right]\left[1 - \left(\frac{r}{R}\right)^2\right]. \qquad (4)$$

Here, $\Delta z = z - z_0$ such that z_0 is the designated entry point of the flow, $\Delta p(z) = p(0,z_0) - p(0,z)$ is the corresponding pressure gradient, and $v_0 = v_z(r = 0, z_0)$ is the axial velocity at the entry point $z = z_0$. In eq. 3, we have replaced the expression $\frac{\lambda}{Re}$ in the original solution by Yuan with $\frac{v_{\mathrm{in}}}{v_0}$, since $\mathrm{Re} = \frac{v_0 R\rho}{\mu}$ and $\lambda = \frac{v_{\mathrm{in}}\rho R}{\mu}$. As can be seen from eq. 4, flow speed is parabolic although the axial velocity v_z keeps increasing with z due to continuous influx of fluid through the walls. Indeed, experiments have reported [31] that cytoplasmic velocity does increase up to the start of the turn, which in our model is located where the cylinder meets the cone.

For sustained oogenesis in *C. elegans* gonad, a volumetric flow rate $Q = 2\pi R L_{\mathrm{cyl}} \times v_{\mathrm{in}}$ of cytoplasm through the rachis tube is maintained near the turn. For this magnitude of Q we can then obtain the pressure difference $\Delta p_{\mathrm{rachis}}$ between the distal end of the gonad and the turn by using eq. 3. Now, how does this $\Delta p_{\mathrm{rachis}}$ compare with the pressure difference Δp_{pipe} required for generating the same Q for regular pipe flow with the boundary influx turned off (Poiseulle flow)? We note that the steady-state velocity profile has the same parabolic form $v_z(r,z) = U(z)[(1 - (r/R)^2]$ in both the cases, where $U(z) = v_z(0,z)$ is the axial velocity along the central axis ($r = 0$). For a non-porous pipe, $U(z) = v_{\mathrm{pipe}}$ is independent of z, whereas for the rachis, $U(z) = v_0[1 + \frac{4v_{\mathrm{in}}}{v_0}\frac{\Delta z}{R}]$, as per the notation described in the text following eq. 4. For the net flux at the turn, $Q(z = L_{\mathrm{cyl}}) = \int_0^R v_z(r, L_{\mathrm{cyl}}) \times 2\pi r dr$, to be same

in both the cases, we need

$$v_{\rm pipe} = v_0 \left[1 + \frac{4v_{\rm in}}{v_0}\frac{(L_{\rm cyl} - z_0)}{R}\right]. \quad (5)$$

Substituting for v_0 from eq. 5 into the formula for pressure drop (eq. 3) we get the pressure drop over distance $L_{\rm cyl}$ as

$$\Delta p_{\rm rachis} = \frac{\Delta p_{\rm pipe}}{2} \quad (6)$$

where, $\Delta p_{\rm pipe} = \frac{4\mu v_0 L_{\rm cyl}}{R^2}$ is the corresponding pressure drop in a plane tube [15]. Thus the rachis flow requires approximately half the pressure head compared to a tube, in order to deliver the same flux. Hence, the rachis flow mechanism seems to have the feature of better maintaining the uniformity of pressure over a given distance when compared with a general pipe flow. On the other hand, pressure difference is needed between the rachis and the germline cells all along the rachis for cytoplasmic influx into the rachis.

To quantify flows in the pre-turn (cylinder) part of the rachis, the only unknown parameter left is $v_{\rm in}$, which is estimated by comparison with the cytoplasmic streaming speeds reported in a few experiments. We use two independent experimental inputs for this purpose and both give similar estimates. For example, the mean axial speed was reported to be maximum at the turn of the rachis and had a magnitude of $\approx 7\ \mu$m/min [31]. By continuity of the incompressible flow, the total influx of fluid from the walls of the cylinder equals the overall volumetric flux Q at the turn, i.e., the intersection between the cylinder and the cone, such that $2\pi R L_{\rm cyl} v_{\rm in} = \pi R^2[\bar{v}(L_{\rm cyl}) - \bar{v}(0)] = \pi R^2 \bar{v}(L_{\rm cyl})$. This condition implies that $v_{\rm in} = \frac{R}{2L_{\rm cyl}}\bar{v}(L_{\rm cyl})$, since $\bar{v}(0) = 0$ at the distal end. Using $\bar{v}(L_{\rm cyl}) \approx 7\ \mu$m/min, as noted above, $v_{\rm in} \approx 0.09\mu$m/min. We can also estimate $v_{\rm in}$ from the fact that an oocyte is produced every 23 minutes [18]. Volume of the oocyte at the end of the rachis is about $\approx 14000\ \mu$m^3. Assuming uniform injection we get $v_{\rm in} \approx 0.05\mu$m/min.

3.2 Fluid pressure and flow in the entire rachis (cylinder and cone)

We now obtain the axisymmetric velocity and pressure profiles in the entire rachis, depicted by the combined cylindrical and conical region. The influx at the cylindrical wall $v_{\rm in} = 0.14\ \mu$m/min is as earlier, and a linearly decaying outflux at the conical wall $v_{\rm out} = v_o(1 - \frac{z}{L})$, where $L = L_{\rm cyl} + L_{\rm cone}$, and v_o is obtained by equating total influx into the cylinder with the total outflux from the cone (see fig. 2). As discussed earlier, we set pressure $p(z = 0) = P_0$ at the left boundary as a proxy for zero flux (see fig. 1b)), and $\mathbf{v}(z = L_{\rm cyl} + L_{\rm cone}) = 0$ at the right boundary for numerical convergence.

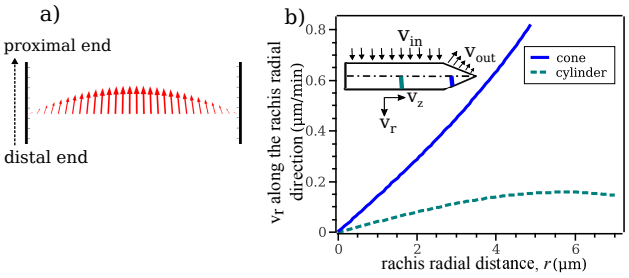

Figure 2. **The parabolic velocity profile of the cytoplasmic fluid flow along the axial direction in the rachis.** a) The red arrows show a parabolic profile and we can see that the fluid flow takes an inward bend near the injection boundary into the axial direction. b) v_r along the rachis radial distance in the cylinder at $z = 180\ \mu$m and, the cone at $z = 300\ \mu$m.

The axisymmetric velocity in the cylindrical portion is shown in fig. 2. As predicted by eq. 4, v_z indeed has a parabolic profile in the cylindrical region. The radial component v_r is negative (due to injection) and small as compared to v_z, and also decays away from the wall ($r = R$) towards the central axis ($r = 0$) (see fig. 2). In the conical portion for which we do not have any analytical formula, v_z is still parabolic while v_r is positive (due to outflux) and rises steeply away from the central axis (see fig. 2). It follows from flow continuity that v_z keeps rising upto the junction where the cylinder meets the cone and decays thereafter. Although the volumetric discharge through the conical cross section keeps decreasing with z due to the cumulative outflux at the walls, v_z could show a local increase along z due to the narrowing of the cross-sectional area. However, for the $v_{\rm out}$ we have chosen, this effect gets suppressed and zero velocity condition is satisfied at the proximal end.

In order to produce mean velocity $\bar{v}$ of approximately a few microns per minute in the rachis, consistent with experimental observation [31], the required pressure drop across the full length of rachis turns out to be very small, ≈ 7 Pa. However, for *C. elegans* the pressure in the internal tissues, which include the gonad tube, is $2 - 30$ kPa [22]. More specifically, Gilpin *et al.* [9] have reported that when the worm is subjected to compression of up to tens of kPa, it resists contraction beyond 30% volumetric strain, which they attributed to the incompressibility of the internal tissues including the gonad tube. They further showed that mutants without the outer cuticle also demonstrate similar resistance to compression. Therefore the cytoplasmic pressure in the rachis is most likely to be in the kPa range. On this scale the drop in pressure along flow direction (few Pa) is negligible. We also estimate later that the reduction in internal cell pressure along the moving train of oocytes is of the order

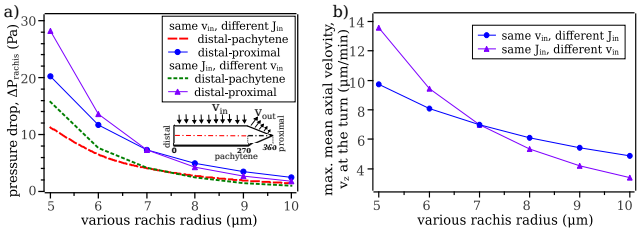

Figure 3. **Variation of net pressure drop and axial velocity as a function of rachis radius.** a) Both cases, i) constant total flux and ii) constant $v_{\rm in}(z)$ show decay of pressure head and, b) axial velocity, v_z with increasing rachis diameter. The broken lines in a) are the analytical results (eq. 3) for pressure drop across the cylindrical region. The symbol and continous line in a) show the computationally obtained pressure drop in the entire rachis from the distal towards the proximal end. Uniform influx and a linearly decaying outflux were used (see inset and main text).

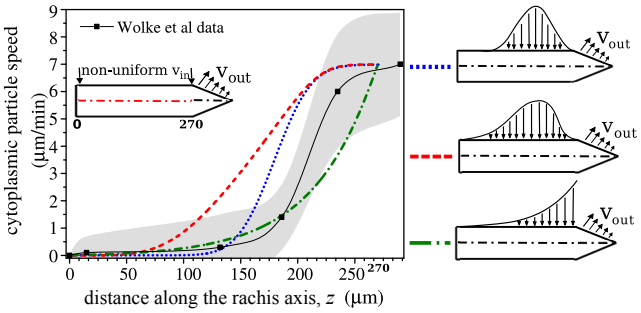

Figure 4. **Cytoplasmic speed inside the rachis: comparison to experiment [31].** Symbols, are the experimental data, along with their error bars (the shaded region). The broken lines are our computation results for the cylindrical region, for different influx profiles $v_{\rm in}(z)$ (qualitatively shown on the side). The various influx velocity functions are blue $\rightarrow$ $v_{i1}\exp(-[\frac{z-z_{i1}}{l_{i1}}]^2)$, red $\rightarrow$ $\frac{v_{i2}}{2}(1-\tanh[\frac{z-z_{i2}}{l_{i2}}])$ and green $\rightarrow$ $v_{i3}\exp(\frac{z-z_{i3}}{l_{i3}})$ and values of the constants used are $z_{i1}=180\ \mu$m, $l_{i1}=35\ \mu$m, $z_{i2}=220\ \mu$m, $l_{i2}=20\ \mu$m, $z_{i3}=20\ \mu$m and $l_{i3}=55\ \mu$m.

of 30 Pa. Thus the pressure in the germ-cells forming the outer lining of the rachis decay faster along the flow direction when compared to the fluid pressure within the rachis. A change in the sign of the pressure difference $p_{\rm cell}-p_{\rm rachis}$ from positive to negative can explain the role reversal of the germline cells from being the feeder of the rachis to being fed by the rachis when they grow into oocytes. Of course, other mechanisms mediated by actin can also add to the lowering of pressure in the oocytes.

The equation for pressure drop in the fluid flow is dependent on rachis dimensions. The rachis width can be widened or narrowed by reducing or increasing, respectively, the contractility of the rachis bridge, as reported in *ani-2* mutants of *C. elegans* [1, 24]. In fig. 3, we show the net pressure drop over the length of the rachis, computed for different rachis radii, keeping the total flux $J_{\rm in}$ same in one case, and $v_{\rm in}$ same in the other. In both cases pressure drop and mean streaming speed decrease with increasing rachis diameter, (see fig. 3). Similar trend for streaming speed was also observed in experiments of ref. [24], although it is not clear which ensemble, constant influx or constant $v_{\rm in}$ is applicable in that case.

In fig. 4, we plot the cytoplasmic particle speed for different regions of the rachis as reported by ref. [31]. The curve is nonlinear, where as our basic model, with uniform influx $v_{\rm in}$, gives a linear mean velocity profile in the cylindrical region. This shows the need for spatially nonuniform injection profile. We explored various forms for the injection and ejection profiles $v_{\rm in}(z)$ and $v_{\rm out}(z)$ which is shown in fig. 4 along with the resulting mean axial speed. In all such variations the total influx (and hence outflux) have been kept same as in the uniform injection case.

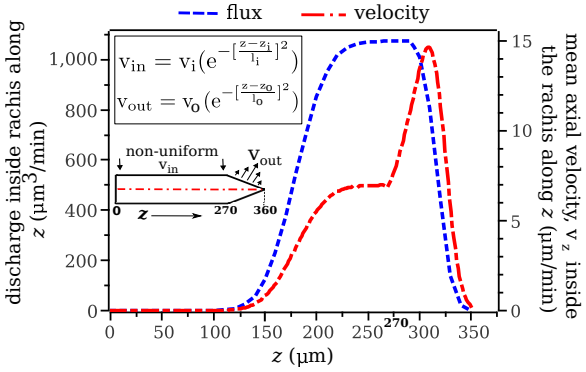

Figure 5. **Cytoplasmic flux and axial speed due to spatially inhomogeneous influx and outflux.** Both $v_{\rm in}(z)$ and $v_{\rm out}(z)$, shown in the legends, are chosen to be Gaussians, centred at the mid-points $z_i=180\mu$m and $z_o=320\mu$m of the cylindrical and conical regions, respectively, with values of the constants $l_i=35\mu$m and $l_o=16\mu$m. Total influx at the cylindrical boundary is equal to the total outflux from the conical wall, and has the same magnitude as that used for fig. 4.

3.3 Experimental and computational estimates for outflux after the turn (cone)

Although we do not directly model the migration of the moving germline cells along the wall of the rachis, we can estimate their speed from experiental data of Wolke *et al.* [31]. For this we track the change in volume of the successive oocytes, ΔV along the rachis in the proximal zone. As the oocytes eject at a rate of one per 23 minutes (=Δt) [18], the successive oocytes trailing in the assembly line move by one cell distance Δs, with a volume change of ΔV. After measuring Δs from experiment images [31] using ImageJ we compute the speed of the oocytes, $v_{\rm cell} = \frac{\Delta s}{\Delta t}$. We do this exercise over consecutive five cells in the proximal region after the turn in the rachis (see fig. 6a) and table 3.3). Berger *et al.* [3] have recently reported the average cell migration speed in the nearby pachytene region to be $0.052\ \mu{\rm m/min}$. Considering the fact that the streaming speed monotonically increases towards the turn and decreases after that, our estimates from the images are quite close.

cell#	ΔV ($\mu{\rm m}^3$)	$J_{\rm out}$ ($\mu{\rm m}^3/{\rm min}$)	Δs (μm)	$v_{\rm cell}$ ($\mu{\rm m/min}$)
1	1566.06	68.09	20.55	0.89
2	797.92	34.69	23.00	1.00
3	2899.89	126.08	26.32	1.14
4	3508.35	152.54	23.33	1.01
5	559.73	24.34	25.44	1.10

Table 1. The estimate of outflux $J_{\rm out}$ with which the streaming cytoplasm fills the oocytes, and the oocyte speed $v_{\rm cell}$ in the direction from late pachytene region towards the proximal end as labelled in the fig. 6a). The volume change in each oocyte during time interval $\Delta t = 23$ minutes of one ovulation cycle is ΔV. The average cell-length and the distance Δs between each oocytes are measured using ImageJ.

We also estimate the cytoplasmic outflux speed $v_{\rm out}$ in the proximal region from the rachis to the growing oocytes using the same data [31], using the relation $\frac{\Delta V}{\Delta t} = v_{\rm out} \times \pi r^2_{\rm rachis}$ for the individual oocytes, where their rate of growth is determined by the influx through the rachis bridge. The radii of the rachis bridges in the oocytes, $r_{\rm rachis}$ are approximated by half of the oocyte length. The values of $J_{\rm out}$, obtained this way, for five successive oocytes (see fig. 6a)) are shown in table 3.3 and shows a spatially inhomogenous profile with z. We therefore also studied the case when both $v_{\rm in}(z)$ and $v_{\rm out}(z)$ are both spatially inhomogeneous. The corresponding spatial profiles for cytoplasmic discharge in the rachis and the average streaming speed are shown in fig. 5. Both axial speed and flux reaches a plateau as the influx tappers off near $z \approx 200\mu$m, but the velocity rises sharply in the range $z = 270 - 310\mu$m as the flow enters the cone (at $z = 270\mu$m) with narrowing cross-section and where the outflux is yet to pick up, but then rapidly decays to zero after peaking.

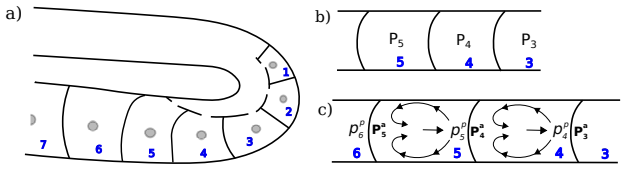

Figure 6. **Schematic of the growing and moving oocytes beyond the gonad turn.** a) The oocytes are labelled for better understanding of their position towards the proximal end in the discussed calculations. Curvature is observed at the interface between adjacent oocytes and can be seen due to b) the pressure difference across them, and c) the pressure gradient developed between the anterior and posterior ends inside the oocytes because of potential cytoplasmic streaming within oocytes.

4 Estimate of pressure gradients in the germline across the oocytes

Fluorescent visualization of oocytes [31] shows that the interface between two successive oocytes has a convex curvature towards the exit implying that the oocytes ahead in the queue have decreasing pressure. Assuming quasistatic conditions, the curvature gives us an estimate for the pressure drop across the interface. From the experimental figures in Wolke *et al.*, [31], we measured the radius of curvature R_c of the successive interfaces between the cells $3, 4, 5$ and 6, as labelled in fig. 6a), by fitting circles to the interfaces using ImageJ (see table 2) – the radius of curvature in the perpendicular direction was also assumed to be R_c (i.e., spherical interface). Ignoring bending rigidity of the cell-cell interfaces, we estimate the pressure drop across cell (see table 2) using the Young-Laplace equation as $\Delta P_{\rm cells} = 2\sigma/R_c$, where, σ is the interfacial surface tension of the order $\sim 3 \times 10^{-4}{\rm N/m}$ [30]. However, the applicability of Young-Laplace equation relies on pressure equilibriation inside the individual cells of interest, an assumption which may not be completely correct since the oocytes are continuously fed by cytoplasm streaming in the rachis. Morever, since the oocytes are moving, a part of this pressure difference across the oocytes may be required to overcome friction between the oocytes and their surroundings. We also note that cytoplasmic streaming that requires a pressure difference of the order $5 - 6$ Pa between the an-

cell interface	R_c (μm)	ΔP_{cells} (Pa)
3↔4	17	35.3
4↔5	17.1	35.1
5↔6	23	26.1
6↔7	28	21.4

Table 2. This table shows the pressure drop across the neighbouring oocytes that are lined up towards the proximal end of the gonad, while cytoplasmic streaming continues (fig. 6b)). The radius of curvature of the cells, R_c is measured from fig. 1B of Wolke *et al.* [31] using ImageJ.

terior and the posterior ends of the cell has been visualised within *C. elegans* one-cell embryo [20]. Since the anterior end of one of the oocytes in the germline is the posterior end of the other, this pressure difference could be another possible reason for the nonzero curvature of the oocyte-oocyte interfaces. In figs. 6b) and c) we show a schematic depicting both these scenarios.

5 Discussion

From the preceding analysis, a simple picture of the oocyte formation process emerges. Germline cells in the distal arm of *C. elegans* gonad, including the apoptotic nurse cells, first squeeze their cytoplasm into the enclosed rachis. Such donation of cytoplasm by nurse cells to the growing ooctyes is also seen during oogenesis in *Drosophila* [27, 25]. The cytoplasmic influx then streams through the rachis and is absorbed by the oocytes in the proximal arm of the gonad. The streaming process, which we model as Stokes flow in a porous tube, is also greatly reminiscent of blood flow through the capillary vessels and glomerular filtration in the kidneys [23, 12]. An interesting feature of this flow mechanism, in which there is a gradual build up of volumetric flow in the rachis through the boundary influx, is its ability to maintain a relative constancy of fluid pressure head within the rachis, when compared with the regular impermeable pipe flow.

The outflux of cytoplasm from the rachis into the oocytes requires the pressure in the rachis to be higher than that in the oocytes. While we estimated the pressure drop across successive oocytes to be of the order of $20 - 30$ Pa, our analysis for cytoplasmic streaming shows that the pressure drop across the whole rachis should only be a few pascals. Thus the fluid pressure in the rachis is practically constant at P_{rachis}. Hence, to ensure the flow of cytoplasm into the oocytes, $P_{\text{rachis}} > P_1 > \ldots > P_5$ (see fig. 6b)). This observation implies that the pressure drop between the rachis and the oocytes should gradually increase towards the proximal end, thus potentially resulting in a larger cytoplasmic influx for the oocytes ahead in the queue. This deduction is partially consistent with the data which shows that the influx indeed rises initially between oocytes 1 and 3, but then later decays towards the proximal end between oocytes 3 and 5 (see table 3.3). However, this decrease could also happen due to some other factors not considered here. For example, a higher pressure difference may be required to pump in more cytoplasm into the oocytes as they reach closer to their maximum size.

It is quite likely that the oocytes have internal cytoplasmic pressure in the range of $10 - 100$ Pa, similar to that measured in most eukaryotic cells [29, 6]. Given that $5 - 6$ convex oocyte-oocyte interfaces can be detected towards the proximal end of the *C. elegans* gonad, we estimated the net pressure drop across oocytes 1 and 5 to be of the order of 100 Pa. Hence, to ensure $P_{\text{rachis}} > P_1 > \ldots > P_5$, the cytoplasmic pressure in the rachis must at least be more than 100 Pa. Indeed, the experimentally observed resistance of the gonad tube under hydrostatic compression [9] is also suggestive of high internal pressure in the rachis. However, we note with caution that this estimate relies on the assumption of pressure equilibrium inside the oocytes and the applicability of Young-Laplace equation to slowly moving interfaces between the oocytes. It is also interesting to note that cytoplasmic streaming, and more specifically, circulation inside oocytes could be an alternative reason behind curved interfaces (see schematic fig. 6). Such circulatory flows are known to create pressure gradients inside *C. elegans* embryo (at its single cell stage) and mouse oocytes [20], with higher pressure at the leading edge (anterior), shown in bold-face in fig. 6c).

In this paper, we have performed analytical calculations, numerical computations, and back-of-the-envelope estimates to get insights into various pressure gradients that are likely to be required for cytoplasmic streaming and oogenesis in *C. elegans* gonad. One of the main drawbacks of the current study is that we do not explicitly include the physics of germline cells and oocytes in our model, but include their effect on cytoplasmic streaming only indirectly via influx and outflux. There also are other aspects that are not considered in our modeling. These include, dynamics of rachis bridges [1, 24], movements of germline cells and oocytes [2], unsteady nature of the cytoplasmic flows, exact geometry of the gonad, potential spatio-temporal variability of the cortical tension in the oocytes, and the role of chemical signalling [19]. Although the inclusion of one or more of these features would indeed make the modeling more comprehensive, it would come at the cost of conceptual clarity. The main message of this work is that the fluid pressure within the rachis tube is almost constant, and it is the pressure difference between the cytoplasm in the rachis and germ cells/oocytes that is most likely the

primary driver of cytoplasmic streaming and oogenesis in *C. elegans* gonad. Although quite simple, we believe that our's is the first attempt to not only quantitatively address this vital biophysical process but also make clear and falsiable hypothesis.

Acknowledgments : We acknowledge Nicolas T. Chartier and Stephan Grill for introducing us to the topic of cytoplasmic streaming in *C. elegans* gonad and sharing their experimental movies with us.

References

[1] R. Amini, E. Goupil, S. Labella, M. Zetka, A. S. Maddox, J.-C. Labbé, and N. T. Chartier. C. elegans anillin proteins regulate intercellular bridge stability and germline syncytial organization. *J Cell Biol*, 206(1):129–143, 2014.

[2] K. Atwell, Z. Qin, D. Gavaghan, H. Kugler, E. J. A. Hubbard, and J. M. Osborne. Mechano-logical model of c. elegans germ line suggests feedback on the cell cycle. *Development*, 142(22):3902–3911, 2015.

[3] S. Berger, E. Lattmann, T. Aegerter-Wilmsen, M. Hengartner, A. Hajnal, X. C. i Solvas, et al. Long-term c. elegans immobilization enables high resolution developmental studies in vivo. *Lab on a Chip*, 18(9):1359–1368, 2018.

[4] A. S. Berman. Laminar flow in channels with porous walls. *Journal of Applied physics*, 24(9):1232–1235, 1953.

[5] A. Beyer, R. Eberhard, N. Piterman, M. O. Hengartner, A. Hajnal, and J. Fisher. A dynamic physical model of cell migration, differentiation and apoptosis in caenorhabditis elegans. In *Advances in Systems Biology*, pages 211–233. Springer, 2012.

[6] G. T. Charras, M. Coughlin, T. J. Mitchison, and L. Mahadevan. Life and times of a cellular bleb. *Biophysical journal*, 94(5):1836–1853, 2008.

[7] B. R. Daniels, B. C. Masi, and D. Wirtz. Probing single-cell micromechanics in vivo: the microrheology of c. elegans developing embryos. *Biophysical journal*, 90(12):4712–4719, 2006.

[8] S. Ganguly, L. S. Williams, I. M. Palacios, and R. E. Goldstein. Cytoplasmic streaming in drosophila oocytes varies with kinesin activity and correlates with the microtubule cytoskeleton architecture. *Proceedings of the National Academy of Sciences*, 109(38):15109–15114, 2012.

[9] W. Gilpin, S. Uppaluri, and C. P. Brangwynne. Worms under pressure: bulk mechanical properties of c. elegans are independent of the cuticle. *Biophysical journal*, 108(8):1887–1898, 2015.

[10] R. E. Goldstein and J.-W. van de Meent. A physical perspective on cytoplasmic streaming. *Interface focus*, 5(4):20150030, 2015.

[11] T. L. Gumienny, E. Lambie, E. Hartwieg, H. R. Horvitz, and M. O. Hengartner. Genetic control of programmed cell death in the caenorhabditis elegans hermaphrodite germline. *Development*, 126(5):1011–1022, 1999.

[12] G. Herschlag, J.-G. Liu, and A. T. Layton. An exact solution for stokes flow in a channel with arbitrarily large wall permeability. *SIAM Journal on Applied Mathematics*, 75(5):2246–2267, 2015.

[13] D. Hirsh, D. Oppenheim, and M. Klass. Development of the reproductive system of caenorhabditis elegans. *Developmental biology*, 49(1):200–219, 1976.

[14] J. Kimble and J. White. On the control of germ cell development in caenorhabditis elegans. *Developmental biology*, 81(2):208–219, 1981.

[15] P. K. Kundu, I. M. Cohen, and D. Dowling. Fluid mechanics 4th, 2008.

[16] C. Margraves, K. Kihm, S. Y. Yoon, C. K. Choi, S.-h. Lee, J. Liggett, and S. J. Baek. Simultaneous measurements of cytoplasmic viscosity and intracellular vesicle sizes for live human brain cancer cells. *Biotechnology and bioengineering*, 108(10):2504–2508, 2011.

[17] H. H. Mattingly, J. J. Chen, S. Arur, and S. Y. Shvartsman. A transport model for estimating the time course of erk activation in the c. elegans germline. *Biophysical journal*, 109(11):2436–2445, 2015.

[18] J. McCarter, B. Bartlett, T. Dang, and T. Schedl. On the control of oocyte meiotic maturation and ovulation incaenorhabditis elegans. *Developmental biology*, 205(1):111–128, 1999.

[19] S. Nadarajan, J. A. Govindan, M. McGovern, E. J. A. Hubbard, and D. Greenstein. Msp and glp-1/notch signaling coordinately regulate actomyosin-dependent cytoplasmic streaming and oocyte growth in c. elegans. *Development*, 136(13):2223–2234, 2009.

[20] R. Niwayama, H. Nagao, T. S. Kitajima, L. Hufnagel, K. Shinohara, T. Higuchi, T. Ishikawa, and A. Kimura. Bayesian inference of forces causing cytoplasmic streaming in caenorhabditis elegans embryos and mouse oocytes. *PloS one*, 11(7):e0159917, 2016.

[21] R. Niwayama, K. Shinohara, and A. Kimura. Hydrodynamic property of the cytoplasm is sufficient to mediate cytoplasmic streaming in the caenorhabiditis elegans embryo. *Proceedings of the National Academy of Sciences*, 108(29):11900–11905, 2011.

[22] S.-J. Park, M. B. Goodman, and B. L. Pruitt. Analysis of nematode mechanics by piezoresistive displacement clamp. *Proceedings of the National Academy of Sciences*, 104(44):17376–17381, 2007.

[23] C. Pozrikidis. Stokes flow through a permeable tube. *Archive of Applied Mechanics*, 80(4):323–333, 2010.

[24] A. Priti, H. T. Ong, Y. Toyama, A. Padmanabhan, S. Dasgupta, M. Krajnc, and R. Zaidel-Bar. Syncytial germline architecture is actively maintained by contraction of an internal actomyosin corset. *Nature communications*, 9(1):4694, 2018.

[25] M. E. Quinlan. Cytoplasmic streaming in the drosophila oocyte. *Annual review of cell and developmental biology*, 32:173–195, 2016.

[26] S. A. Raiders, M. D. Eastwood, M. Bacher, and J. R. Priess. Binucleate germ cells in caenorhabditis elegans are removed by physiological apoptosis. *PLoS genetics*, 14(7):e1007417, 2018.

[27] L. R. Serbus, B.-J. Cha, W. E. Theurkauf, and W. M. Saxton. Dynein and the actin cytoskeleton control kinesin-driven cytoplasmic streaming in drosophila oocytes. *Development*, 132(16):3743–3752, 2005.

[28] T. Shinar, M. Mana, F. Piano, and M. J. Shelley. A model of cytoplasmically driven microtubule-based motion in the single-celled caenorhabditis elegans embryo. *Proceedings of the National Academy of Sciences*, 108(26):10508–10513, 2011.

[29] M. P. Stewart, J. Helenius, Y. Toyoda, S. P. Ramanathan, D. J. Muller, and A. A. Hyman. Hydrostatic pressure and the actomyosin cortex drive mitotic cell rounding. *Nature*, 469(7329):226, 2011.

[30] O. Thoumine, O. Cardoso, and J.-J. Meister. Changes in the mechanical properties of fibroblasts during spreading: a micromanipulation study. *European Biophysics Journal*, 28(3):222–234, 1999.

[31] U. Wolke, E. A. Jezuit, and J. R. Priess. Actin-dependent cytoplasmic streaming in c. elegans oogenesis. *Development*, 134(12):2227–2236, 2007.

[32] S. Yuan, A. Finkelstein, and N. Brooklyn. Laminar pipe flow with injection and suction through a porous wall. *Tr ASME*, 78:719–724, 1956.